

# Effects of Boron and Zirconium on the Microstructure and High-Temperature Strength of Cast Fe<sub>3</sub>Al-Based Alloys

M. Rajabi<sup>1</sup>, M. Shahmiri<sup>1</sup>, M. Ghanbari<sup>1,\*</sup>

<sup>1</sup>*School of Metallurgy and Materials Engineering, Iran University of Science and Technology, Tehran, Iran.*

*Received: 20 February 2017 - Accepted: 15 April 2017*

## Abstract

In this study, the effects of boron (B) and zirconium (Zr) on the microstructure and high-temperature strength of Fe<sub>3</sub>Al-based alloys were investigated. Alloying was performed in a vacuum induction melting furnace (VIM) and, consequently, the melt then was poured into a cast iron mold. Microstructural investigation was conducted using optical and electron microscopy, X-ray diffraction, and differential thermal analysis. Addition of B and Zr to the alloys resulted in the formation of boride precipitates and Laves phases. Dendritic microstructures were found in as-cast alloys because of segregation of alloying elements into the interdendritic regions. To evaluate the high-temperature mechanical properties of the alloys, hot pressure test was performed. The results showed that, Zr exhibited the most pronounced effect on the high-temperature strength because of the formation of Laves phases. Boride phases tend to coarsen when increasing the temperature to 650°C, and they have no effect on the high-temperature strength of the alloy. In the temperature range of 450°C–550°C, an anomaly in the temperature-dependence of the yield strength was observed.

**Keywords:** Iron aluminides, Boron, Zirconium, Yield stress, Casting, Microstructure.

## 1. Introduction

Increasing the efficiency of gas engines is a way to reduce the CO<sub>2</sub> and other harmful contamination in the environment. High temperature alloys such as nickel and cobalt based superalloys and other new developed materials are used to improve the efficiency of the gas turbine engines. Iron aluminides with D0<sub>3</sub> ordered crystal structure exhibit good resistance to hot corrosion and hot sulfidation, and are lower in cost compared with other high-temperature alloys [1-4]. Fe<sub>3</sub>Al-based alloys have a density of 5.4–6.7 g/cm<sup>3</sup>, which is approximately 30% lower than those of stainless steels and Ni-based superalloys, and have a good strength-to-weight ratio. In addition, the development and application of these classes of materials would decrease the use of strategically important elements such as Cr and Ni [5-7]. Although, iron aluminides have low strength at high temperatures and low ductility at low temperatures, which limit the use of this type of material, their mechanical properties can be improved by the addition of proper alloying elements [8-10].

It has been reported that one of the most important reasons for the embrittlement of iron aluminides is hydrogen embrittlement as a result of moisture in the environment. Environmental embrittlement can be decreased by the addition of Cr [10]. Because of the D0<sub>3</sub> ordered crystal structure of Fe<sub>3</sub>Al-based aluminides, good mechanical properties are expected until the critical stability temperature of

the D0<sub>3</sub> phase is reached. At temperatures higher than the D0<sub>3</sub>-B<sub>2</sub> transition temperature, a degradation of the mechanical properties of these aluminides is observed [9]. There are several methods to improve the mechanical properties of iron aluminides including solid solution strengthening and Laves, boride, and carbide-precipitate hardening [10-12]. Because of a low solid-state solubility of boron (B) and zirconium (Zr) in Fe<sub>3</sub>Al, boride precipitates and laves phases tend to form at grain boundaries and in the interior of grains. When B is present in the alloy, Fe<sub>2</sub>B precipitates are formed at grain boundaries. On the other hand, the presence of Zr results in the formation of Laves phases in the alloy and causes high-temperature strengthening [12-20]. The co-existence of B and Zr leads to the formation of ZrB<sub>2</sub>, which acts as an inoculant and refines the grain structure of the alloy [8,10,12] and changes the predominant fracture mode from intergranular to transgranular.

Kratochvíl et al. investigated the effects of C and Zr on the high-temperature mechanical properties of iron aluminides [12]. Large amounts of Laves λ<sub>1</sub>, (Fe,Al)<sub>2</sub>Zr, and ZrC precipitates were observed in their investigations. The formation of Laves phases during the deformation of these aluminides affected their high-temperature mechanical properties. The effect of ZrB<sub>2</sub> precipitates on the mechanical properties of iron aluminides was also investigated. It was found that the alloy strength increased up to 600°C, and its ductility was improved [8].

Stein et al. evaluated the effect of Zr on Fe–Al alloys and showed that Zr addition leads to an increase in the volume fraction of Laves phases in

\*Corresponding author

Email address: ghanbari@iust.ac.ir

the alloys, which improves the high-temperature mechanical properties of the alloys [14].

In the present study, the effects of B and Zr on the microstructure and high-temperature mechanical properties of cast Fe<sub>3</sub>Al-based alloys were systematically investigated.

## 2. Materials and Methods

Chemical compositions of the alloys used in this study are presented in Table 1. Pure ingots of iron (99.95 wt.%), aluminum (99.99 wt.%), Cr (99.99 wt.%), Zr (99.99 wt.%), and Al–B master alloy (8 wt.% B) were used to produce the alloys. Melting was performed using a vacuum induction melting furnace with an alumina crucible. The melt was then poured into a preheated cast iron mold. Cylindrical samples with a diameter of 40 mm and height of 200 mm were produced.

The microstructure and mechanical properties of the alloys were evaluated in the as-cast condition. Optical microscopy (OM-MEIJ) and scanning electron microscopy (SEM-TESCAN) in combination with energy-dispersive spectrometry (EDS) microanalysis were used to evaluate the microstructure and chemical composition of phases. The samples were polished using SiC abrasive papers and finally using diamond paste with 0.1- $\mu$ m particle size. The samples were then chemically etched using an etching reagent containing 1% HF, 33% CH<sub>3</sub>COOH, 33% HNO<sub>3</sub>, and 33% H<sub>2</sub>O. X-Ray Diffraction (XRD) technique was performed to evaluate phases formed in as-cast samples. A Cu cathode with a wavelength of 1.54 Å, scanning rate of 1°C/s, and 2 $\theta$  range of 2°–100° was used for XRD measurements. Differential thermal analysis (DTA; STA-504) was used to determine critical phase transition temperatures for D0<sub>3</sub>–B<sub>2</sub> and B<sub>2</sub>–A<sub>2</sub> transitions. The samples were placed in an alumina crucible under argon and heated at a rate of 10°C/min with a precision of  $\pm$ 1°C. Compression tests were performed at room temperature and higher temperatures (precision  $\pm$ 1°C) using an Instron 4208 testing device at a strain of 10<sup>-4</sup>·S<sup>-1</sup>.

The samples were prepared according to the ASTM E208 standard (9 mm height and 6 mm diameter).

**Table 1. Nominal compositions (at.%) of Fe<sub>3</sub>Al-based alloys used in this study.**

Alloy designation	Al	Cr	Zr	B	Fe
A	27.8	2	0	0.5	Bal.
B	28.3	1.8	0.5	0	Bal.
C	28.6	1.9	0.5	0.5	Bal.

## 3. Results and Discussion

### 3.1. Microstructural and Phase analysis

Optical micrographs revealed a dendritic structure with precipitates in the interdendritic regions.

Fig. 1a shows an optical micrograph of the as-cast alloy A, from which it can be seen that there exists a dendritic Fe<sub>3</sub>Al matrix and a Fe<sub>3</sub>Al–Fe<sub>2</sub>B eutectic structure with lamellar morphology. Boron has low solid-state solubility in Fe<sub>3</sub>Al; therefore, during solidification, it draws back from the solidification front and precipitates as Fe<sub>3</sub>Al–Fe<sub>2</sub>B eutectic structure in the interdendritic regions. This causes an increase in the strength at the grain boundaries [10]. It was reported that during heat treatment of Fe<sub>3</sub>Al alloys, the eutectic structure is dissolved, and the lamellar Fe<sub>3</sub>Al–Fe<sub>2</sub>B structure converts to a Fe<sub>2</sub>B phase with spherical morphology (after homogenization at 1200°C for 48h) [10].

As shown in Fig. 1b, the microstructure of the alloy B is dendritic with interdendritic precipitates. As found for B, Zr has low solid-state solubility in Fe<sub>3</sub>Al and forms a  $\lambda_1$  Laves phase, (Fe,Al)<sub>2</sub>Zr, which has a major effect on the high-temperature properties of Fe<sub>3</sub>Al alloys [12–16]. Interdendritic Laves phases could be formed as lamellar phases, continuous phases, and as very fine precipitates in the grains.

In alloy C, a cooperative effect on the microstructure due to the presence of both B and Zr is observed, as shown in Fig. 1c Zr reacts with B in the alloy and forms the ZrB<sub>2</sub> phase. The ZrB<sub>2</sub> phase refines the grain structure of the alloy and improves

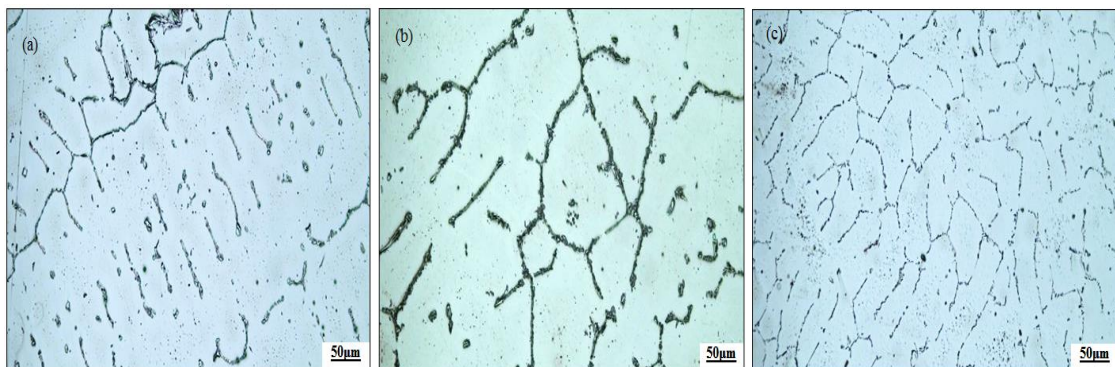


**Fig. 1. OM images of as-cast alloys: a) A, b) B, and c) C. The alloy compositions are given in Table 1.**

its ductility [8,10,12]. It is also expected that  $\lambda_1$  Laves phases precipitate in the interdendritic regions as a result of the Zr concentration being higher than the B concentration.

Kratochvíl et al. reported that if the Zr:B atomic ratio is greater than one,  $\lambda_1$  Laves phases are the major precipitated phases, and only a small amount of  $ZrB_2$  will be formed. For Zr:B atomic ratios less than one, the major precipitated phase is  $ZrB_2$ , and no  $\lambda_1$  Laves phases will be formed [12]. Generally, the Zr:B atomic ratio in  $Fe_3Al$  alloys will determine the type of precipitates. Increasing the concentration of B and Zr in  $Fe_3Al$  alloys resulted in increment of constitutional under cooling and caused the formation of finer secondary dendritic arms and refined the final microstructure [8, 14].

SEM micrographs of as-cast samples are shown in Fig. 2. The morphology of precipitated phases is shown. The precipitates are mainly formed at the grain boundaries and so, they can strengthen the grain boundaries.

Fig. 3. shows the EDS mapping of the Zr-containing alloy, in which it can be seen that Zr is mainly

concentrated in the precipitates. On the other hand, Cr is distributed uniformly throughout the matrix, which indicates that Cr is soluble in  $Fe_3Al$  alloys [19-22].

Cr is an important alloying element that improves the ductility of alloys based on  $Fe_3Al$ . In fact, two main factors affect the ductility of  $Fe_3Al$  alloys:

1. The dissolution of Cr causes changes in atomic arrangements and increases the number of anti-phase boundaries (APBs) in superdislocations. This leads to a decrease in the energy of the APBs and eases the movement of superdislocations, in turn causing them to cross-slip.

2. Cr incorporation changes the surface condition of the alloy by creating a passive layer of  $Cr_2O_3$ , which prevents H atom diffusion and thus decreases the embrittlement of the alloy [22].

Fig. 4. shows the XRD patterns of the alloys where  $Fe_3Al$ , boride precipitates, and Laves phases can be identified. Because of the low volume fraction of borides and Laves phases, the relevant peaks are weak and difficult to analyze.

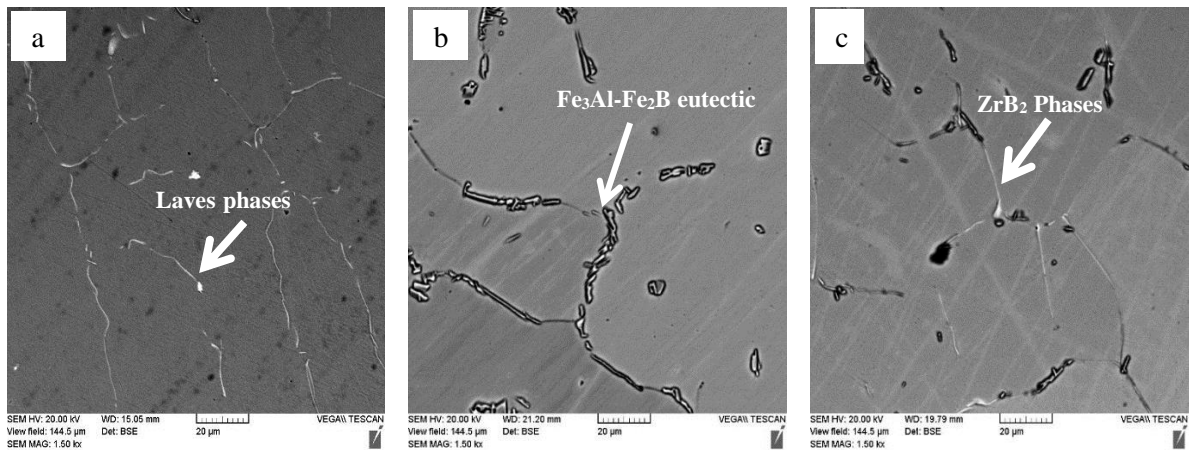


Fig. 2. SEM images of as-cast alloys: a) A, b) B, and c) C. The alloy compositions are given in Table 1.

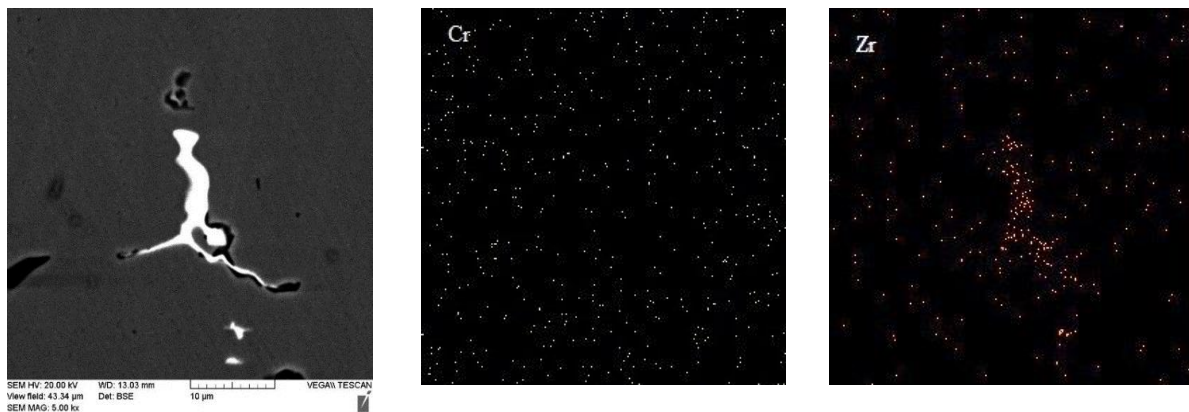


Fig. 3. X-ray mapping showed the distribution of Zr and Cr in  $Fe_3Al$  alloy.

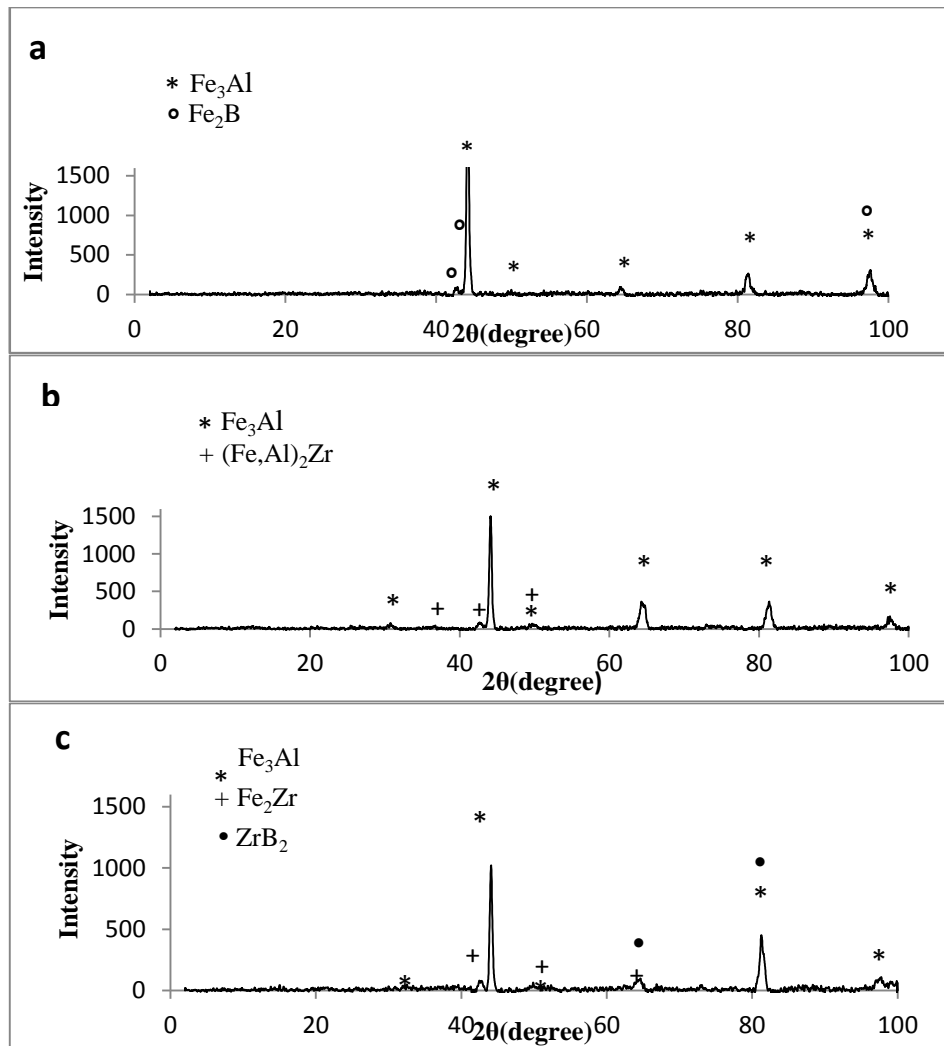


Fig. 4. XRD patterns of as-cast alloys: a) A, b) B, and c) C. The alloy compositions are given in Table 1.

### 3.2. DTA Results

The results of DTA tests are shown in Table 2. The critical temperatures of the  $D0_3$ - $B_2$  and  $B_2$ - $A_2$  phase transitions were determined. The critical transition temperatures are affected by the chemical composition of the alloys, and the precipitates have no effect on them [19]. This demonstrates that B and Zr have no effect on the phase transition temperatures.

Anthony and Fultz showed that variation of the  $D0_3$ - $B_2$  transition temperature is related to the atomic radii of Al and the solute atoms. In fact, when the difference in atomic radii between Al and the solute atoms is small, the elastic energy of the crystal structure is low, so the  $D0_3$ -ordered crystal structure is more stable [23]. As a result of the low solubility of B and Zr in the matrix, and large atomic radius difference between Al and B or Zr, these alloying elements have little or no effect on the transition temperatures of  $Fe_3Al$ -based alloys [10,19,23]. All of the reasons for the variation of critical temperature for the  $D0_3$ - $B_2$  transition also

apply to the  $B_2$ - $A_2$  transition. Alloying elements such as Ti, Mo, W, and Nb, with high solid-state solubility and similar atomic radii to Al, increase the critical temperatures of the phase transitions [19,23].

Table 2. Transition temperatures for ordering transformation by DTA.

Alloy No.	$T_{C}^{D0_3-B_2}(^{\circ}C)$	$T_{C}^{B_2-A_2}(^{\circ}C)$
A	557	897
B	559	896
C	561	900

### 3.3. High-Temperature Compression Tests

The effect of temperature on the work softening of the alloy is depicted in Fig. 5. It can be seen that by increasing the temperature, the maximum strength and toughness of the alloys are decreased. These phenomena are more pronounced at temperatures higher than the  $D0_3$ - $B_2$  transition ( $650^{\circ}C$ ). The variation in the yield strength of the alloys with temperature is depicted in Fig. 6. Increasing the

temperature decreases the yield point of the alloys. The decrement in yield strength at 650°C is more severe for alloy A, which has the lowest strength of the alloys. Boride phases cause an increase in the strength of the grain boundaries and thus increase the strength of the alloy [17].

Up to 550°C, alloy A has the highest strength; however, this alloy has the lowest strength at 650°C. This may be a result of the activation of more slip systems as temperature increases, which would ease the movement of dislocations. Alloy B experiences the smallest drop in strength at 650°C and alloy C, which contains both B and Zr, has a greater strength than alloy A. The effect of Zr on the high-temperature strength of the Fe<sub>3</sub>Al-based alloys is obvious at 650°C, which is the creep service condition of these alloys, and the difference in the strength of alloy B between room temperature and 650°C is about 53 MPa.

The presence of Laves phases at the grain boundaries and inside the grains has little effect on the high-temperature strength of the alloy. However, during deformation of the alloy at high temperatures, nanometric meta-stable Laves phases, (Fe<sub>1-x</sub>Al<sub>x</sub>)<sub>3</sub>Zr and Fe<sub>2</sub>Zr, will be formed in the matrix and interact with dislocations, preventing them from moving easily [12]. In alloy C, B and Zr form ZrB<sub>2</sub> phases in the interdendritic regions and decrease the volume fraction of Laves phases in the microstructure. On the other hand, ZrB<sub>2</sub> phases cause grain refinement and improve the ductility of the alloy [10,12].

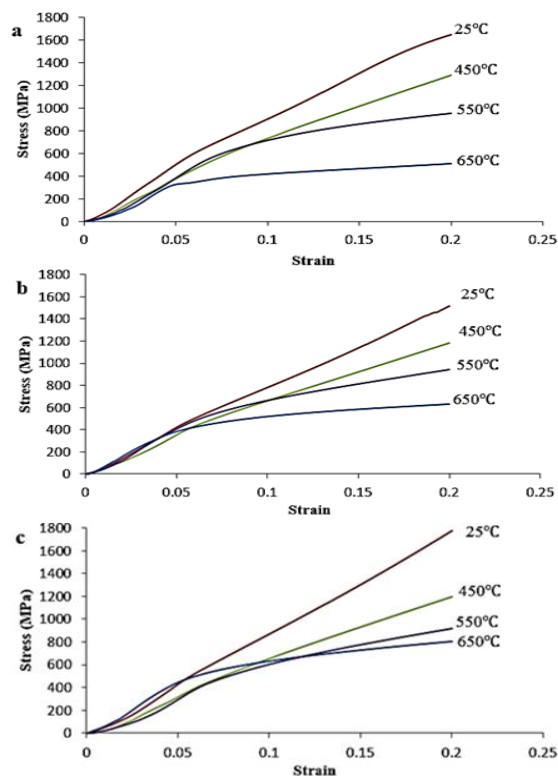


Fig. 5. Flow curves of alloys at various temperatures: a) A, b) B, and c) C.

An anomaly in the variation of yield point with temperature exists for alloys B and C. When increasing the temperature from 450°C to 550°C, the yield strength increases. This phenomenon is common for Fe<sub>3</sub>Al-based alloys [19,24]. In alloy A, this phenomenon was not observed. The reason for this is not obvious, but there have been several investigations in this field, and various theories exist, such as conversion of dislocation structure, in which  $\langle 111 \rangle$  superdislocations are converted to  $\langle 100 \rangle$  perfect dislocations [25], climb locking of  $\langle 111 \rangle$  super dislocations [26-28], and, as recently reported by Morris [24], the presence of thermal vacancies in Fe<sub>3</sub>Al-based alloys, which are immobile and interact with dislocations, prevents dislocation movement. Alternatively, at temperatures in the range 500°C–700°C, the number of vacancies increases and causes the anomaly in the yield strength. By increasing the temperature, vacancies would become more mobile and their pinning effect would increase so that the yield strength of the alloy would drop [24].

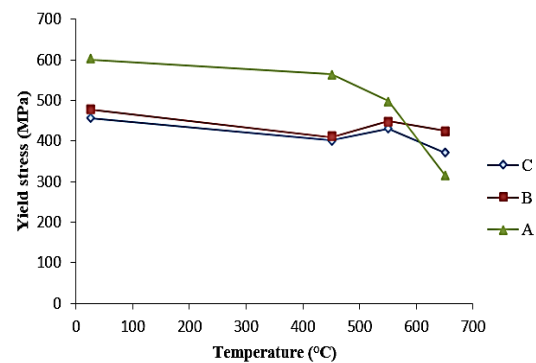


Fig. 6. Dependence of yield strength on temperature for different alloys.

#### 4. Conclusions

1. The structure of as-cast Fe<sub>3</sub>Al-based alloys is dendritic. B and Zr form boride and Laves phases in the interdendritic regions and have no effect on the critical D0<sub>3</sub>-B<sub>2</sub> and B<sub>2</sub>-A<sub>2</sub> phase transition temperatures.
2. Because of Laves phase formation, Zr has a considerable effect on the high-temperature strength. Fe<sub>3</sub>Al-based alloys containing Zr as an alloying element have the greatest yield strength at 650°C. The reason for this phenomenon is not the large number of initial Laves phases in the microstructure, but the nanometric metastable Laves phases that form during high-temperature deformation.
3. Boride phases tend to coarsen when increasing the temperature to 650°C, and have no effect on the high-temperature strength of the alloy. In the temperature range 450°C–550°C, an anomaly in the temperature-dependence of the yield strength was observed.

## References

- [1] D.G. Morris, *Intermetallics*, 6(1998), 753.
- [2] N.S. Stoloff, C.T. Liu, *Intermetallics*, 2(1994), 75.
- [3] N.S. Stoloff, *Mater. Sci. Eng. A*, 258(1998), 1.
- [4] G. Sauthoff: *Intermetallics*, VCH Verlagsgesellschaft, Weinheim, (1995), 65.
- [5] W.C. Luu, J.K. Wu, *Mater. Chem. Phys.*, 70(2001), 236.
- [6] K.V.edula: *Intermetallic compounds*, Vol. 2, John Wiley & Sons Ltd., Chichester, (1994), 199.
- [7] D.D. Risanti, G. Sauthoff, *Intermetallics*, 19(2011), 1727.
- [8] D.G. Morris, M.A. Muñoz-Morris, *Mater. Sci. Eng. A*, 462(2007), 45.
- [9] M. Palm, *Intermetallics*, 13(2005), 1286.
- [10] R. Krein, A. Schneider, G. Sauthoff and G. Frommeyer, *Intermetallics*, 15(2007), 1172.
- [11] P. Kratochvíl, P. Kejzlarb, R. Krála and V. Vodicková, *Intermetallics*, 20(2012), 39.
- [12] P. Kratochvíl, F. Dobeš, J. Pešička, P.Málek, J. Buršík, V. Vodičková and P. Hanus, *Mater. Sci. Eng. A*, 548(2012), 175.
- [13] X. Li, P. Prokopčáková and M. Palm, *Mater. Sci. Eng. A*, 611(2014), 234.
- [14] F. Stein, M. Palm and G. Sauthoff, *Intermetallics*, 13(2005), 1275.
- [15] P. Kratochvíl, P. Málek, M. Cieslar, P. Hanus, J. Hakl and T. Vlasák, *Intermetallics*, 15(2007), 333.
- [16] A. Wasilkowska, M. Bartsch, F. Stein, M. Palm, K. Sztwiertnia, G. Sauthoff and U. Messerschmidt, *Mater. Sci. Eng. A*, 380(2004), 9.
- [17] P. Lejček, A. Fraczkiewicz, *Intermetallics*, 11(2003), 1053.
- [18] J.W. Cohron, Y. Lin, R.H. Zee and E. P. George, *Acta Mater.*, 46(1998), 6245.
- [19] F. Stein, A. Schneider and G. Frommeyer, *Intermetallics*, 11(2003), 71.
- [20] D.A. Alven, N.S. Stoloff, *Mater. Sci. Eng. A*, 239-240(1997), 362.
- [21] D.A. Alven, N.S. Stoloff, *Scripta Mater.*, 34(1996), 1937.
- [22] Y.D. Huang, W.Y. Yang and Z.Q. Sun, *Intermetallics*, 9(2001), 119.
- [23] L. Anthony, B. Fultz, *Acta Metall. Mater.*, 43(1995), 3885.
- [24] D.G. Morris, M.A. Muñoz-Morris, *Intermetallics*, 13(2005), 1269.
- [25] H. Xiao, I. Baker, *Scripta Metall. Mater.*, 28(1993), 1411.
- [26] J.T. Guo, O. Jin, W.M. Yin and T.M. Wang, *Scripta Metall. Mater.*, 29(1993), 783.
- [27] K. Yoshimi, S. Hanada and M.H. Yoo, *Acta Metall. Mater.*, 43(1995), 4141.
- [28] M.H. Yoo, J.A. Horton and C.T. Liu, *Acta Metall.*, 36(1988), 2935.